FLYING WING AERODYNAMIC ANALYSIS

Vasile PRISACARIU*, Ionică CÎRCIU, Mircea BOŞCOIANU****

*"Transilvania" University, Brasov, **"Henri Coandă" Air Force Academy

***Abstract**: Integrating innovative solutions in the construction of the UAV is one of the research trends in the field having direct influence on the performance of unmanned airborne systems. The aerodynamic concepts applied to the UAV disregard the human component – the overload factor limit, but are still dependent on performance (aerodynamic coefficients of buoyancy - C_z and of the drag - C_x) as well as on the breaking boundaries of the UAV structures.*

***Keywords**: flying wing, vortex lattice method, morphing concept, longitudinal stability , lateral stability.*

1. INTRODUCTION

UAV field is constantly expanding both in terms of constructive solutions and the missions they may fulfill. If, in the beginning, the use of UAVs was solely military, they now have a wide use in civilian areas. The main motivation for using this type of aircraft is the low cost of construction and operation compared to manned aircraft. The creation of aerodynamic forces which sustain the aircraft during flight is influenced by the physical properties of the surrounding air mass. Therefore, we can say that specialists successfully apply the same concepts, principles and methods used in aeronautical manned aircraft. The field of fluid movement uses UAV-related concepts such as gravity and its effects, air viscosity and aircraft influence at different flight speeds, the speed of sound in various fluid media (gas, liquid), types of fluid flow on a solid surface (laminar, vortex) and its effects (separation of air fillets, boundary layer), the effects on the flow on wings with DHS (great-sustentation devices - flaps, leading edge flap), aerodynamic profile, airfoil, finite span wing and their polar diagrams, rotary wing and blade element (helicopters, auto-gyros), aircraft progression along the trajectory (takeoff, ascension, gliding, landing, stunt flying), balance, loading, stability, maneuverability (Russell, 1996). The evolution of unmanned aircraft included the development of air vectors of the flying wing type (tailless) due to low production and operating costs and to the ease of use. Aeronautics imposed three sets of flying wings in terms of achieving stability: straight wings (plank), arrow wings (swept) and parafoil wing. Flying wings are operational in several types of robotic aerial systems (UAS Yearbook, 2011) which successfully perform data acquisition missions both for civilian use and in military operations (see fig.1).

Fig.1 Robotic aerial systems - Flying wing type. a. EADS, Germany (plank) b. EagleScan, USA (swept) c. Snowgoose, Canada (parafoil)

2. FLYING WING ANALYSIS

The analyzed wing is the bilongeron wing (with tubular fiberglass longerons) with plywood ribs at recess and at extreme profile. It is made of EPS (Expanded Polystyrene) presenting the security features listed in Table 2. The wing consists of two half-planes that

are mounted together in a dihedral angle of 0^0. We propose to analyze a bearing area (fig. 2) having the Clark YH profile and the input data specified in Table 1.

Table 1 Flying wing data

Span	*2b*	2000 mm	*Aspect ratio*	λ	8,00
Main chord	c_0	350 mm	*Weight*	*G*	0,50 kg
Medium aerod. chord	*MAC*	263.33 mm	*Surface*	*S*	0,50 m^2

Table 2 EPS data

Data	EPS 15	EPS 20
Density (kg/m^3)	15	20
Elasticity modulus (N/mm^2)	4	4,7
Breaking strain (N/mm^2)	0,24	0,27
Stretch rezistance (N/mm^2)	0,19	0,27

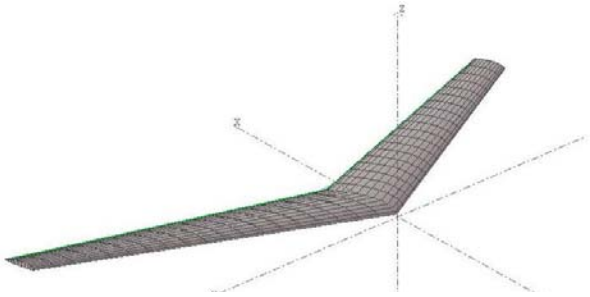

Fig.2. Flying wing for analysis

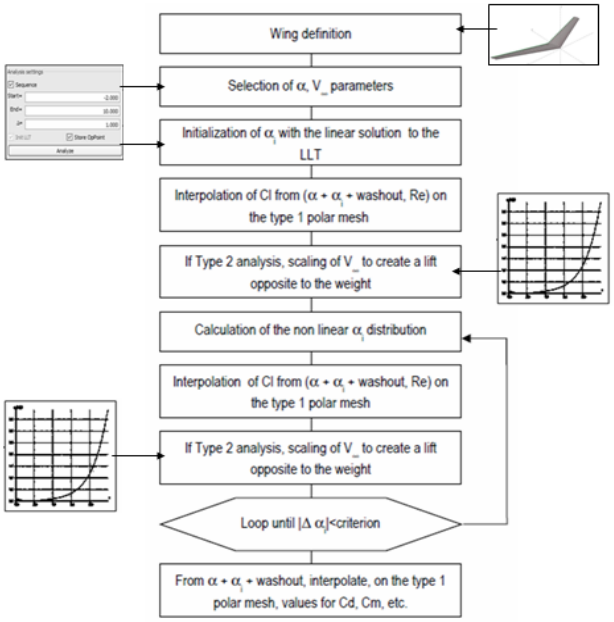

Fig.3 Representation of the polar diagram (*Guidelines for XFLR5*, 2011)

Methodology and analysis tools. XFLR5 is software that enables 2D and 3D aerodynamic analysis of bodies and bearing areas, separately or jointly. The software makes analysis for small Reynolds numbers. The latest version has implemented five applications: a direct 2D analysis and design, a 3D analysis and design (wing, fuselage, aircraft), two ways to design and compare 2D, design a 2D QDES and MDES. According to XFLR5 manual (*Guidelines for XFLR5*, 2011), the steps in fig.3 should be taken into account when developing polar diagrams appropriate to the input data.

Fig.3 shows the analyzed wing based on the characteristics in Table 1 and its bearing, drag, and induced resistance diagram in accordance with figures 4, 5 and 6 through VLM method (vortex lattice method) that involves a certain degree of accuracy of the analysis.

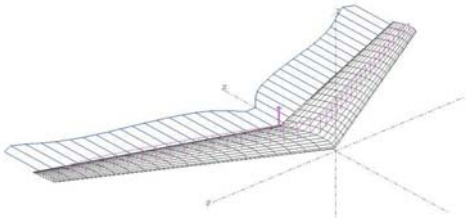

Fig.4 Lifting and drag diagram (72 km/h and 5^0 incidence)

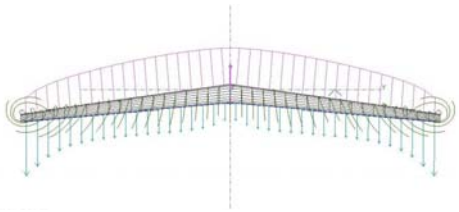

Fig.5 Lifting anf induce drag diagram (72 km /h and 12^0 incidence)

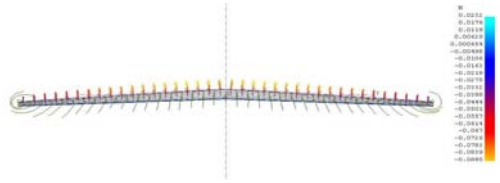

Fig. 6 Wing forces and induce drag (36 km/h and 5^0 incidence)

Table 3 shows the values obtained depending on the angle of incidence for the proposed wing.

Table 3. The coefficients depending on the angle of incidence

Data points = 21

alpha	CL	ICd	PCd	TCd	CY	Cn	Rn	Yn	IYn	QInf	XCP
-4.000	-0.200234	0.001678	0.000000	0.001678	0.000000	-0.019935	-0.000000	-0.000000	-0.000000	20.0000	0.3581
-4.000	-0.119836	0.000641	0.000000	0.000641	0.000000	-0.018868	-0.000000	-0.000000	-0.000000	20.0000	0.3649
-3.000	-0.039935	0.000068	0.000000	0.000068	0.000000	-0.017798	-0.000000	-0.000000	-0.000000	20.0000	0.3907
-2.000	0.040718	0.000072	0.000000	0.000072	0.000000	-0.016838	-0.000000	-0.000000	-0.000000	20.0000	0.3878
-1.000	0.123770	0.000606	0.000000	0.000606	0.000000	-0.015897	-0.000000	-0.000000	-0.000000	20.0000	0.3624
0.000	0.204770	0.001488	0.000000	0.001488	0.000000	-0.014838	-0.000000	-0.000000	-0.000000	20.0000	0.3613
1.000	0.286668	0.003224	0.000000	0.003224	0.000000	-0.013741	-0.000000	-0.000000	-0.000000	20.0000	0.3607
2.000	0.366404	0.005808	0.000000	0.005808	0.000000	-0.012648	-0.000000	-0.000000	-0.000000	20.0000	0.3604
3.000	0.448898	0.007898	0.000000	0.007898	0.000000	-0.011560	-0.000000	-0.000000	-0.000000	20.0000	0.3602
4.000	0.527210	0.010990	0.000000	0.010990	0.000000	-0.010439	-0.000000	-0.000000	-0.000000	20.0000	0.3601
5.000	0.607176	0.014577	0.000000	0.014577	0.000000	-0.009306	-0.000000	-0.000000	-0.000000	20.0000	0.3599
6.000	0.686780	0.018647	0.000000	0.018647	0.000000	-0.008161	-0.000000	-0.000000	-0.000000	20.0000	0.3598
7.000	0.765977	0.023191	0.000000	0.023191	0.000000	-0.007008	-0.000000	-0.000000	-0.000000	20.0000	0.3598
8.000	0.844716	0.028196	0.000000	0.028196	0.000000	-0.005847	-0.000000	-0.000000	-0.000000	20.0000	0.3597
9.000	0.922945	0.033647	0.000000	0.033647	0.000000	-0.004679	-0.000000	-0.000000	-0.000000	20.0000	0.3596
10.000	1.000629	0.039530	0.000000	0.039530	0.000000	-0.003506	-0.000000	-0.000000	-0.000000	20.0000	0.3596
11.000	1.077729	0.045828	0.000000	0.045828	0.000000	-0.002329	-0.000000	-0.000000	-0.000000	20.0000	0.3595
12.000	1.154146	0.052523	0.000000	0.052523	0.000000	-0.001150	-0.000000	-0.000000	-0.000000	20.0000	0.3595
13.000	1.229885	0.059596	0.000000	0.059596	0.000000	0.000030	-0.000000	-0.000000	-0.000000	20.0000	0.3594
14.000	1.304902	0.067026	0.000000	0.067026	0.000000	0.001209	-0.000000	-0.000000	-0.000000	20.0000	0.3594
15.000	1.379140	0.074792	0.000000	0.074792	0.000000	0.002385	-0.000000	0.000000	0.000000	20.0000	0.3593

Figure 6 shows the bearing coefficient variation all along the chord for an angle of incidence of 5^0 and a speed of 20 m / s while Figure 7 and 8 shows the variation of the induced angle as well as of the pressure centre line at 5^0 incidence.

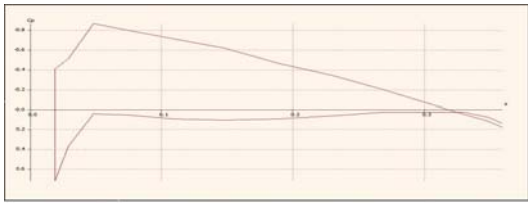

Fig. 7. Lifting coefficient variation along the chord

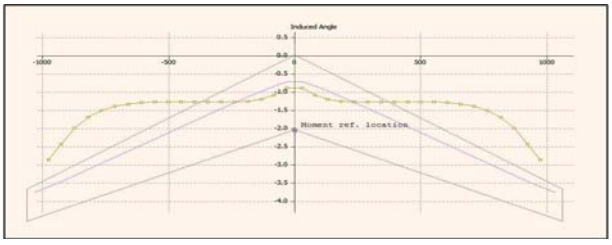

Fig. 8. Induced angle and pressure centre line

3. DINAMIC STABILISATION ANALYSIS

Lateral normal- modes. In most cases, the equation of the lateral linear system (1) admits a negative real root, relatively high in mode (an a-periodic mode with high damping) and a small real root, negative or positive (a slow damped or ascending a-periodic mode) and a pair of complex conjugate roots with negative real part (oscillator short-term mode) - Figure 9. The rapid a-periodic mode plays the most important part in the deviation of the rolling p angular velocity or of the side angle φ with the name rapid convergent depreciation of roll. The slow a-periodic mode (the spiral mode) is the most important in the law of angle variation of lateral inclination and φ of azimuth ψ, the aircraft describing a spiral in the horizontal plane. The oscillator mode characterizes the skidding angle β and the angular velocities p and r (Grigore, 1987).

$$A \cdot \lambda^5 + B \cdot \lambda^4 + C \cdot \lambda^3 + D \cdot \lambda^2 + E \cdot \lambda = 0 \qquad (1)$$

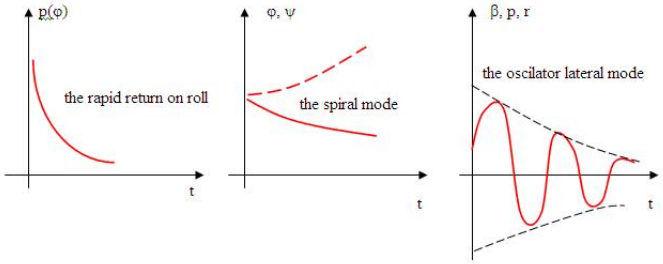

Fig. 9. Lateral normal-mode graphics

3D analysis and asymetrical calculations. Calculation case. The stability analysis follows the following steps in figure 10.

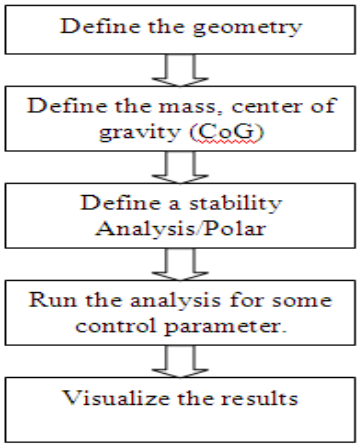

Figure 10. Steps of the stability analysis

Control and stability analysis actually means evaluating the response time of an aircraft to the disturbances of a flight of constant equilibrium. These disturbances may

occur due to environmental factors or to the control area. The following mathematical representation is possible by means of simplifying conditions: Neumann boundary conditions are used.

Position of the weight centre	Inertia instances
CoG_x= 350.5690 mm CoG_y= 0.0000 mm CoG_z= 13.5961 mm	Ibxx= 1.051e+05 kg.mm² Ibyy= 1.255e+04 kg.mm² Ibzz= 1.176e+05 kg.mm² Ibxz= 255.5 kg.mm²

Problem solving (software calculation steps)

Calculation for control position -2.00
Creating the influence matrix...
Performing LU Matrix decomposition...
Solving LU system...
Searching for zero-moment angle... Alpha=13.65005°
Creating source strengths...
Calculating doublet strength...ut
Calculating speed to balance the weight...
VInf = 3.68013m/s
Calculating the stability derivatives
No active control - skipping control derivatives

Longitudinal derivatives	*Lateral derivatives*
Xu= -0.12674	Yv= -0.0028088
Cxu= -0.11245	CYb= -0.0024922
Xw= 0.91477	Yp= 0.29526
Cxa= 0.81166	CYp= 0.26198
Zu= -2.6693	Yr= -0.075793
Czu= -0.0032135	CYr= -0.06725
Zw= -4.5007	Lv= -0.36153
CLa= 3.9934	Clb= -0.16039
Zq= -0.47264	Lp= -1.0156
CLq= 3.1851	Clp= -0.45055
Mu= 1.1185e-09	Lr= 0.70044
Cmu= 3.7686e-09	Clr= 0.31074
Mw= 0.021324	Nv= 0.087976
Cma= 0.071848	Cnb= 0.03903
Mq= -0.095688	Np= -0.42611
Cmq= -2.4487	Cnp= -0.18904
Neutral Point position= 345.83119mm	Nr= 0.0063622 Cnr= 0.0028225

State matrix

Longitudinal state matrix	Lateral state matrix
-0.2534 1.8295 0 -9.81 -5.3385 -9.001 2.734 0 8.911e-08 1.69-7.623 0 0 0 1 0	-0.0056 0.590 -3.83 9.81 -3.442 -9.526 6.631 0 0.8296 -3.425 -0.095 0 0 1 0 0

Control matrix

Longitudinal control matrix	Lateral control matrix
0 0 0 0	0 0 0 0

Initial conditions

$$\varphi = 0 \qquad u_0 = 5\frac{m}{s} \qquad w_0 = 5\frac{m}{s} \qquad q_0 = 1^0 s$$

Figures 11 and 12 exemplify the graphs representing variations in speed *d* along axes x and z as well as the variations in time of the speed along axis z and of the rotation around axis x.

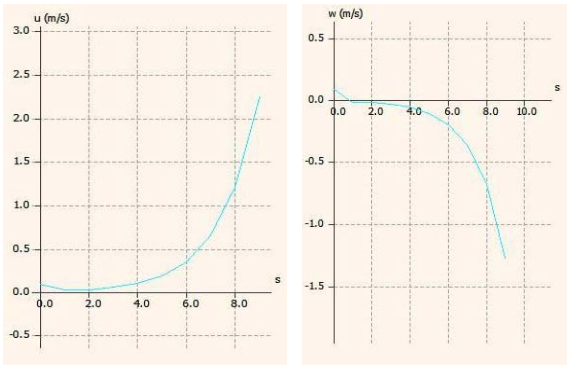

Fig. 11. Variations in time of the speeds along axes x and z (longitudinal stability)

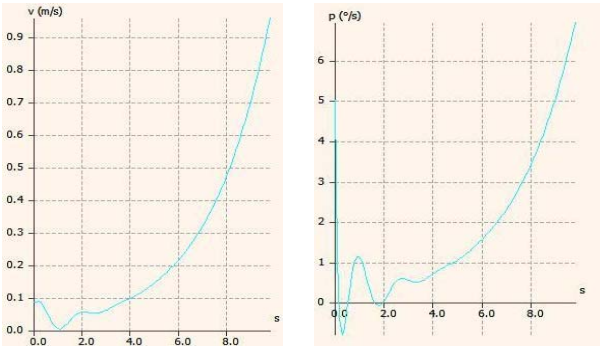

Fig. 12. Variations in time of the speed along axis z and of the rotation around axis x

The display of the results regarding speed variation in time and rotation angle variation in relation to axis x, in case of longitudinal stability, according to figure 13.

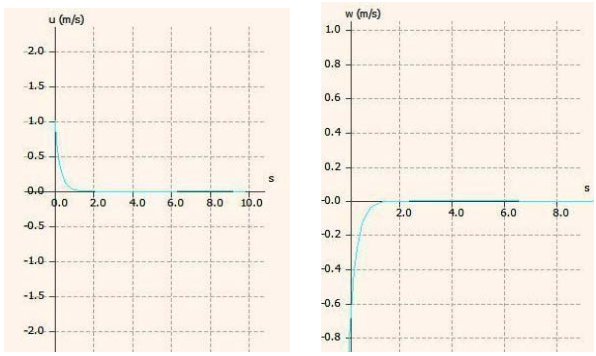

Fig. 13. Speed variations in time and rotation angle variation in relation to axis x

The display of the results regarding speed variation in time and rotation angle variation in relation to axis x, in case of lateral stability, according to figure 14.

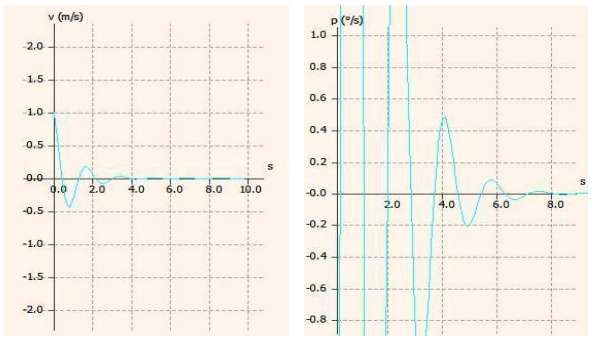

Fig. 14. Speed variations in time and rotation angle variation in relation to axis x

4. CONCLUSIONS

In conclusion, during disturbed lateral movement, the aircraft moves in a neutral way in relation to one of the degrees of freedom of this movement because the equation (4) has at least one null solution. No aircraft flying in a in a straight and uniform manner will maintain a constant azimuth direction after a disturbance; it will tend towards a new direction of flight depending on the size of the disturbance. Disturbed lateral movement of an aircraft with blocked controls presents the following features: *the idle mode,* which is a constant deviation after each lateral disturbance of the azimuth angle ψ; *the fast a-periodic mode*, which is a rapid depreciation lateral tilt; *the spiral-mode*, which is a slow a-periodic motion (easy to control), *the lateral oscillator mode (Dutch roll),* which is a rapid oscillatory motion and it must be a stable and rapidly amortized mode.

Using inertial sensors to measure the characteristics of the response to flight maneuvers along with the qualitative analysis of the performance lead to an overall improvement of the flying wing aerodynamics.

5. ACKNOWLEDGMENT

The authors wish to thank “Transylvania” University and "Henri Coandă" Air Force Academy of Braşov for supporting the research necessary for writing this article.

BIBLIOGRAPHY

1. Grigore, I. (1987). *Aircraft Flight Mechanics.* Bucharest: Military Academy Publishing House.
2. Russell, J.B. (1996). *Performance and stability of aircraft.* London.
3. ***. (2009). *Surfaces – User Manual – Vortex-Lattice Module.* Great OWL Publishing – engineering software.
4. ***. (2011). *Guidelines for XFLR5 v6.03*.
5. ***. (2011). *UAS Yearbook. Unmanned aircraft systems – The Global Perspective 2011/2012*. Paris: Blyenburg & Co.